Breaking the Symmetry between Interaction and Replacement in Evolutionary Dynamics on Graphs

Hisashi Ohtsuki,[1,2] Martin A. Nowak,[1,3] and Jorge M. Pacheco[4]

[1]*Program for Evolutionary Dynamics, Harvard University, Cambridge Massachusetts 02138, USA*
[2]*Department of Biology, Faculty of Sciences, Kyushu University, 6-10-1 Hakozaki, Fukuoka 812-8581, Japan*
[3]*Department of Organismic and Evolutionary Biology, Department of Mathematics, Harvard University, Cambridge, Massachusetts 02138, USA*
[4]*Centro de Física Teórica e Computacional, Departamento de Física da Faculdade de Ciências, P-1649-003 Lisboa Codex, Portugal*

(Received 3 January 2007; published 8 March 2007)

We study the evolution of cooperation modeled as symmetric 2×2 games in a population whose structure is split into an interaction graph defining who plays with whom and a replacement graph specifying evolutionary competition. We find it is always harder for cooperators to evolve whenever the two graphs do not coincide. In the thermodynamic limit, the dynamics on both graphs is given by a replicator equation with a rescaled payoff matrix in a rescaled time. Analytical results are obtained in the pair approximation and for weak selection. Their validity is confirmed by computer simulations.

DOI: 10.1103/PhysRevLett.98.108106 PACS numbers: 87.23.−n, 87.23.Kg, 89.75.Fb

The availability and characterization of data specifying the networks of contacts between individuals [1,2] has spurred a renewed interest in the study of dynamical processes in structured populations [1–16]. In this context, evolutionary game dynamics constitutes a widely used framework, from physics to political science [1–16]. Traditionally, evolutionary game dynamics involves the replicator equation, describing deterministic dynamics in infinite populations [17]. In finite populations, stochastic effects cannot be overlooked [18,19], and many insights have been gained recently by bridging the gaps between stochastic and deterministic dynamics and between finite and infinite populations [20–22] (for a review, see [15]).

However, population structure is often more complex than that emerging from a single static graph description [1]. Individuals do not usually rely on a single network to carry out their decisions. Decision making is often based on additional information about the interacting partner, obtained via networks which rarely overlap perfectly with the network of interactions. Similarly, our role models are seldom those we have the possibility to interact with regularly. Finally, our network of close friends often bears little resemblance with the network of our professional relations, similarly to what one observes in the animal world, where grooming and other manifestations of close relationship are usually established among kin, despite the fact that often fitness is acquired via interaction with the non-kin. Hence, study of dynamical processes in more than a single network constitutes an important ingredient neglected so far, which is relevant to other processes such as rumor spreading, traffic regulation, epidemic modeling, etc. In this work we explore a first step toward the inclusion of more sophisticated layers of population structure, explicitly distinguishing two types of graphs defining contacts between individuals: the interaction graph, H, determines who-meets-whom in an evolutionary game; the replacement graph, G, specifies evolutionary updating or, in the context of cultural evolution, defines who-is-the-role-model-of-whom. Both graphs have the same vertices, where each vertex is occupied by one individual. There are no empty vertices. The graphs H and G can differ in their edges. Hence, we break the symmetry between these two types of graphs, compared to the more traditional approach, in which they coincide. This simple model allows us to explore the new features associated with this richer and more powerful representation of population structure, and also allows us to derive approximate analytical results whose validity is assessed by means of computer simulations. It will be concluded that, whenever the symmetry between graphs H and G is broken, it is harder for cooperators to thrive compared to the case when the two graphs coincide. More realistic implementations should also take into account that strategies and structure coevolve with variable time scales [23,24].

Let us consider social dilemmas associated with symmetric 2×2 games between two pure strategies, cooperators C and defectors D. The entries of the matrix $\mathbf{\Phi}$ represent the payoffs for the row player:

$$\begin{array}{c} \\ C \\ D \end{array} \begin{array}{c} \begin{array}{cc} C & D \end{array} \\ \begin{pmatrix} R & S \\ T & P \end{pmatrix} \end{array}. \tag{1}$$

R is the reward for mutual cooperation, P is the punishment for mutual defection, T is the temptation to defect, and S is the sucker's payoff. Different orderings of the payoff values define well-known social dilemmas: The prisoner's dilemma (PD) ($T > R > P > S$), the snowdrift game (SG) ($T > R > S > P$), and the stag-hunt game ($R > T > P > S$) [8].

Each individual uses either strategy C or D, which he plays with all his neighbors in the interaction graph H, accumulating a total payoff Π. The fitness is given by $F = 1 - w + w\Pi$. Here $0 \leq w \leq 1$ represents the relative

contribution of the game to fitness. If $w = 1$ then the payoff is equal to fitness ("strong selection"). If $w = 0$ then the game is irrelevant for fitness; all players have the same fitness ("neutral drift"). We shall study the limit of "weak selection" [18], $w \ll 1$, which can be justified as follows: First, in most real life situations we are involved in many different games, and each particular game only makes a small contribution to our overall performance. Second, weak selection leads to important analytic insights which are often not possible otherwise (Ref. [19] is an exception). Simulations suggest that these results are good approximations for larger values of w [9]. Updating dynamics proceed on graph G. Following Ref. [9] we adopt death-birth (DB) updating: A random individual is chosen to die; the g neighbors in the replacement graph compete for the empty site proportional to their fitness. Reproduction can be genetic or cultural. In general, however, different update mechanisms lead to different outcomes [25,26]. Details of the present framework and its extension to other update mechanisms and to games in infinite structured populations, involving an arbitrary (finite) number of strategies will be published elsewhere [26].

In a population of size N, the quantity to consider is the fixation probability, defined as the probability that a mutant invading a population of $N - 1$ resident individuals will produce a lineage which takes over the whole population [18,27,28]. We denote the fixation probability of strategy X ($= C$ or D) in a Y population ($= D$ or C, respectively) by ρ_X. For a neutral mutant $\rho_X = 1/N$.

If $\rho_C > 1/N$, then natural selection favors the fixation of strategy C. To derive an analytical result for the fixation probabilities, we resort to the diffusion approximation under weak selection, e.g., $Nw \ll 1$ with $N \gg \max\{g, h\}$, where g, h, and l are defined in Fig. 1. Let x_X denote the global density of strategy X. Let T_C^+ (T_C^-) be the probability that the number of C strategists increases (decreases) by one in each update event. The probability $\phi_C(y_C)$ that strategy C ultimately takes over the whole population, when its initial frequency is y_C, is given as the solution of the backward Kolmogorov equation [29]

$$0 = m(y)\frac{d\phi_C(y)}{dy} + \frac{v(y)}{2}\frac{d^2\phi_C(y)}{dy^2}, \tag{2}$$

where $m(x_C) = T_C^+ - T_C^-$ is the mean of the increment of x_C per unit time and $v(x_C) = (T_C^+ + T_C^-)/N$ is the variance of the increment of x_C per unit time. From this equation, the fixation probability is calculated as $\rho_C = \phi_C(1/N)$. Hence, we need to calculate T_C^+ and T_C^-.

Clearly, the state of the population can no longer be described in terms of global densities of strategies, x_C and x_D (mean-field approximation). In each configuration of the population, each vertex can have either a C or a D individual. There are 2^N possible configurations, a huge number for large N. Here we adopt the pair-approximation method [30,31] to describe the local configurations of strategies on graphs, which considers not only frequencies of strategies, but also frequencies of (connected) strategy pairs and enables us to estimate the correlation of strategies in adjacent nodes. We have three different types of pairs: those connected only through G, those connected only through H, and those connected through both graphs. We label each of them (G), (H), or (L), respectively.

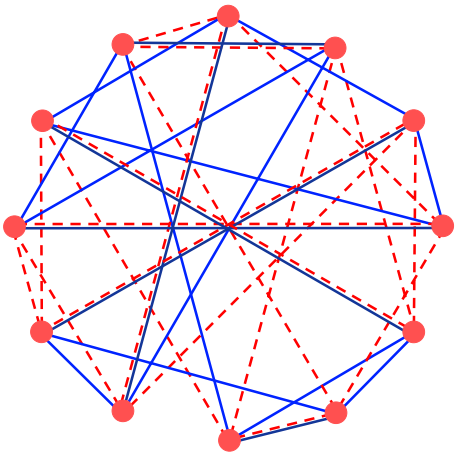

FIG. 1 (color online). Solid blue lines belong to the interaction graph H, with connectivity h; dashed red lines belong to the replacement graph G, with connectivity $g \geq 3$; double lines (dashed red and solid blue) define the overlap graph L, with connectivity l. In the example shown, all graphs are random and homogeneous [32]. The procedure to generate them is straightforward: given values of h, g, l, we start by constructing a random regular graph [32] of degree g, ensuring that it is connected. Subsequently, we augment this graph by increasing the connectivity of all nodes by $h - l$, such that G has connectivity g, H has connectivity h, and L has connectivity l.

Let $q_{X|Y}$ be the conditional probability that the focal node is occupied by strategy X given that strategy Y occupies the adjacent node. This conditional probability depends on the type of edges connecting X and Y. Therefore, we need to distinguish $q_{X|Y}^{(G)}$, $q_{X|Y}^{(H)}$, and $q_{X|Y}^{(L)}$. In the weak selection limit, we expect these "local" conditional probabilities to equilibrate much faster than global frequencies of strategies, x_X, since the latter will equilibrate at a speed of order w. Hence, the system reaches a local steady state characterized by the following values, independent of the update dynamics [26]

$$q_{X|Y}^{(H)} = x_X, q_{X|Y}^{(G)} = q_{X|Y}^{(L)} = \frac{g-2}{g-1}x_X + \frac{1}{g-1}\delta_{X,Y}. \tag{3}$$

It is obvious that correlations between two adjacent nodes build up only through G, and not via H. Hence, the local conditional probability $q_{X|Y}^{(H)}$ is given by its global frequency, x_X. Regarding the other edges, (G) and (L), with probability $1/(g-1)$ a player shares a common ancestor with his neighbor. With the remaining probability, $(g-2)/(g-1)$, his neighbor is a random individual. From Eq. (3) we can calculate T_C^+ and T_C^-. For DB updating the condition $\rho_C > 1/N$ leads to the equation

$$g^2h(R + 2S - T - 2P) > gl(2S - 2R + P - T) + l(S - R - P + T), \quad (4)$$

and

$$\rho_C > \rho_D \Leftrightarrow (gh + l)(R - P) > (gh - l)(T - S). \quad (5)$$

Let us now apply the general results above to the two-parameter PD; a cooperator, C, pays a cost c for every edge, and the partner of this edge receives a benefit $b > c$. Defectors, D, pay no cost and distribute no benefits. Hence, $T = b$, $R = b - c$, $P = 0$ and $S = -c$. We find that $\rho_C > 1/N > \rho_D$ if

$$\frac{b}{c} > \frac{hg}{l}. \quad (6)$$

The inequality above, which is valid for DB updating only [26], suggests that for fixed b and c, the optimum configuration for evolution of cooperation occurs when $h = g = l$. The degree l of the overlap should be as large as possible, while the degrees h and g should be as small as possible. This optimum is reached when the replacement graph and the interaction graph are identical. In this limit we recover our previous condition, $b/c > k$ (using $k = h = g = l$) [9]. Any deviation from the identity between graphs H and G makes evolution of cooperation more difficult. Note also that cooperation is never favored if the overlap is empty ($l = 0$). Furthermore, Eq. (6) is symmetric in g and h. Therefore, a highly connected G (large g) and a sparsely connected H (small h) have the same threshold as the reverse situation (for a fixed overlap l).

The results obtained, however, strongly depend on the game under study. Let us now discuss the SG [4], parameterized in terms of costs and benefits. In the SG a cooperator pays a cost c, but two cooperators share this cost. Whenever one player cooperates, both receive a benefit $b > c$. Hence, $T = b$, $R = b - c/2$, $S = b - c$ and $P = 0$. Now the condition $\rho_C > 1/N$ leads to $b/c > [5/2 - x - x/(2g)]/[2 + x - x/g]$, and becomes always easier to fulfill than $\rho_C > \rho_D$ which now reads $b/c > (3 - x)/(2 + 2x)$, where $x = l/gh$. Similarly to the PD, selection will be more favorable to cooperators if the overlap is maximized. Unlike the PD, however, cooperators may now become advantageous even if the overlap l is zero. Furthermore, $\rho_C > 1/N$ is no longer symmetric in g and h: As a result, it is better to have more role models than interaction partners in the SG.

The pair approximation is only valid for infinite Bethe lattices (or Cayley trees) where each node has exactly the same number of links without loops or leaves. However, it was found in Ref. [9] that, under weak selection, pair-approximation works extremely well for random regular graphs and other structures, despite deviations found for scale-free graphs. We shall test Eq. (6) by means of numerical simulations for the PD on random regular graphs [32], which lead to population structures such as those in Fig. 1.

The results are shown in Fig. 2. An excellent agreement is obtained. In particular, simulations confirm the invariance of the condition above upon exchange of h and g. Finite size effects account for the rigid shift of ≈ 0.018 toward lower values of c/b for $N = 100$ and of ≈ 0.0035 for $N = 500$ between the simulation results and the theoretical predictions, which suggest a $1/N$ dependence and an overall insensitivity to the specific values of g, h, and l. Hence, as the population size increases, the agreement between the pair-approximation-based predictions and computer simulations improves.

In practice, for a given finite value of N we need b/c to be slightly larger than the thresholds predicted by our analytical calculations.

Finally, we discuss the implications of breaking the symmetry between H and G in the thermodynamic limit. When $N \to \infty$ the description becomes deterministic, since $v(y) \to 0$ as $1/N$. Hence, the rate of change of x_C is given by $\dot{x}_C = T_C^+ - T_C^-$. Here we shall discuss the results for 2×2 games, although the main results remain valid for m

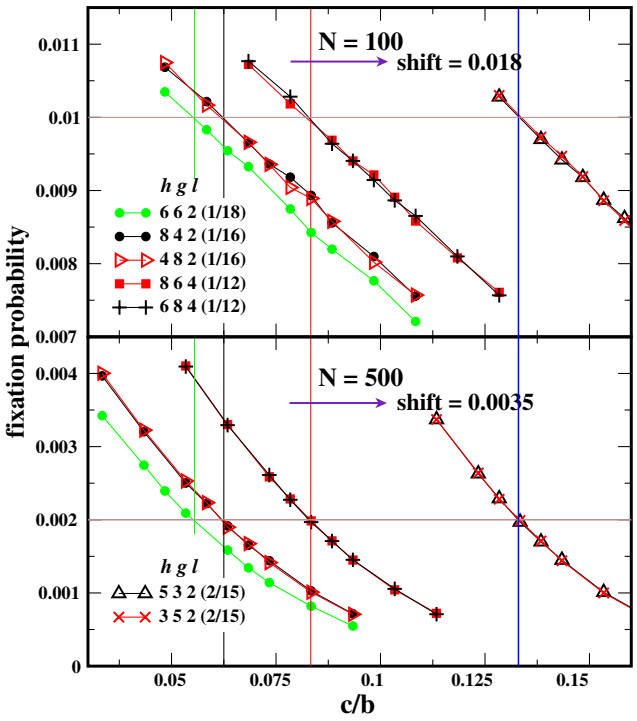

FIG. 2 (color online). Analytical versus numerical calculation of fixation probabilities. We consider populations of size $N = 100$ (upper panel) and $N = 500$ (lower panel). We generate 3×10^3 graphs G and H compatible with fixed (h, g, l), and run 5×10^3 simulations for each graph. We compute the average fixation probability of a single cooperator in a population of defectors. The intersection between vertical lines and the horizontal lines at $1/N$ provide the values predicted analytically by Eq. (6), given in brackets, for each triplet h, g, l. Symbols provide the results of numerical simulations. Note that all data sets have been rigidly shifted by the amounts indicated in the panels, reflecting the finite size effects which scale as $1/N$. Color and line symbols are the same in both panels ($w = 0.1$).

strategies interacting via general $m \times m$ symmetric games [26], for which the replicator equation in a well-mixed population reads [13],

$$\dot{x}_i = x_i(\boldsymbol{e_i} \cdot \boldsymbol{\Phi x} - \boldsymbol{x} \cdot \boldsymbol{\Phi x}), \tag{7}$$

$i = 1, \cdots, m$, where $\boldsymbol{e_i}$ is the ith unit column vector, whereas $\mathbf{x} = (x_1, \cdots, x_m)^T$. For the social dilemmas defined in Eq. (1) and keeping only the linear terms in w in $T_C^+ - T_C^-$ (weak selection) we obtain [33]

$$\dot{x_C} = \tau x_C[\boldsymbol{e_C} \cdot (\boldsymbol{\Phi} + \boldsymbol{\Psi})\boldsymbol{x} - \boldsymbol{x} \cdot (\boldsymbol{\Phi} + \boldsymbol{\Psi})\boldsymbol{x}], \tag{8}$$

where the matrix $\boldsymbol{\Psi}$ reads

$$\begin{array}{c} \\ C \\ D \end{array} \begin{array}{c} \begin{array}{cc} C & D \end{array} \\ \begin{pmatrix} 0 & \sigma \\ -\sigma & 0 \end{pmatrix} \end{array}; \qquad \sigma = \frac{l[(g+1)R + S - T - (g+1)P]}{g^2 h - (g+2)l}, \tag{9}$$

and the time scale constant reads $\tau = w(g-2) \times [g^2 h - (g+2)l]/[g^2(g-1)]$. Equation (8) has precisely the form of a replicator Eq. (7) with time rescaled by the constant τ and an effective payoff matrix given by $\boldsymbol{\Phi} + \boldsymbol{\Psi}$. Naturally, the matrix $\boldsymbol{\Psi}$ will depend on the update mechanism employed, although this matrix is always antisymmetric, even in the case of $m \times m$ games with $m > 2$ [26].

To summarize, breaking the symmetry between interaction and replacement graphs makes it harder for cooperation to evolve in the prisoner's dilemma in which, for cooperation to thrive, it is important that our interaction partners are also our role models. In the limit of weak selection, and making use of the pair approximation, we provide simple conditions under which a cooperator becomes advantageous when immersed in a population of defectors. Comparison with exact computer simulations shows that, apart from population size effects, which scale as $1/N$, the analytical conditions fit nicely the numerical results. In infinite, structured populations, and for weak selection, strategies evolve according to a replicator equation. The effect of population structure is now to induce a transformation of the payoff matrix which affects solely its off-diagonal elements. Once such a transformation is performed, then evolution proceeds "as if" the population were well mixed (unstructured).

Support from the Japan Society for the Promotion of Science (H. O.), the John Templeton Foundation and the NSF/NIH joint program in mathematical biology (NIH Grant No. 1R01GM078986-01) (M. A. N.) and FCT-Portugal (J. M. P.) is gratefully acknowledged. The Program for Evolutionary Dynamics at Harvard University is sponsored by Jeffrey Epstein.

[1] D. J. Watts, Nature (London) **445**, 489 (2007); *Small Worlds* (Princeton University, New Jersey, 1999).
[2] S. N. Dorogovtsev and J. F. F. Mendes, *Evolution of Networks: From Biological Nets to the Internet and WWW* (Oxford University, Oxford, 2003).
[3] H. Ebel and S. Bornholdt, Phys. Rev. E **66**, 056118 (2002).
[4] C. Hauert and M. Doebeli, Nature (London) **428**, 643 (2004).
[5] C. Hauert and G. Szabó, Am. J. Phys. **73**, 405 (2005).
[6] F. C. Santos and J. M. Pacheco, Phys. Rev. Lett. **95**, 098104 (2005).
[7] T. Antal, S. Redner, and V. Sood, Phys. Rev. Lett. **96**, 188104 (2006).
[8] F. C. Santos, J. M. Pacheco, and T. Lenaerts, Proc. Natl. Acad. Sci. U.S.A. **103**, 3490 (2006).
[9] H. Ohtsuki *et al.*, Nature (London) **441**, 502 (2006).
[10] Wen-Xu Wang *et al.*, Phys. Rev. E **74**, 021107 (2006).
[11] Zhi-Xi Wu *et al.*, Phys. Rev. E **74**, 056113 (2006).
[12] P. Holme and G. Ghoshal, Phys. Rev. Lett. **96**, 098701 (2006).
[13] H. Ohtsuki and M. A. Nowak, J. Theor. Biol. **243**, 86 (2006).
[14] C. P. Roca, J. A. Cuesta, and A. Sánchez, Phys. Rev. Lett. **97**, 158701 (2006).
[15] G. Szabó and G. Fath, Phys. Rep. (to be published).
[16] M. A. Nowak, *Evolutionary Dynamics: Exploring the Equations of Life* (Harvard University, Cambridge, MA, 2006).
[17] J. Hofbauer and K. Sigmund, *Evolutionary Games and Population Dynamics* (Cambridge University Press, Cambridge, England, 1998).
[18] M. A. Nowak *et al.*, Nature (London) **428**, 646 (2004).
[19] A. Traulsen, M. A. Nowak, and J. M. Pacheco, Phys. Rev. E **74**, 011909 (2006).
[20] J. C. Claussen and A. Traulsen, Phys. Rev. E **71**, 025101 (2005).
[21] A. Traulsen, J. C. Claussen, and C. Hauert, Phys. Rev. Lett. **95**, 238701 (2005).
[22] A. Traulsen, J. C. Claussen, and C. Hauert, Phys. Rev. E **74**, 011901 (2006).
[23] F. C. Santos, J. M. Pacheco, and T. Lenaerts, PLoS Comput. Biol. **2**, 1284 (2006).
[24] J. M. Pacheco, A. Traulsen, and M. A. Nowak, Phys. Rev. Lett. **97**, 258103 (2006).
[25] M. Nakamaru, H. Nogami, and Y. Iwasa, J. Theor. Biol. **194**, 101 (1998); **240**, 475 (2006).
[26] H. Ohtsuki, J. M. Pacheco, and M. A. Nowak [J. Theor. Biol. (to be published)].
[27] C. Taylor *et al.*, Bull. Math. Biol. **66**, 1621 (2004).
[28] L. A. Imhof and M. A. Nowak, J. Math. Biol. **52**, 667 (2006).
[29] W. J. Ewens, *Mathematical Population Genetics* (Springer, New York, 2004), Vol. 1.
[30] H. Matsuda *et al.*, Springer Lecture Notes in Biomathematics Vol. 71, 154 (2004).
[31] M. van Baalen, in *The Geometry of Ecological Interactions: Simplifying Spatial Complexity*, edited by U. Dieckmann, R. Law, and J. A. J. Metz (Cambridge University Press, Cambridge, England, 2000), p. 359.
[32] F. C. Santos, J. F. Rodrigues, and J. M. Pacheco, Phys. Rev. E **72**, 056128 (2005).
[33] The pair-approximation was used only in obtaining $T_C^+ - T_C^-$.